Ambipolar acceleration of ions in a magnetic nozzle

Alexey V. Arefiev and Boris N. Breizman
Institute for Fusion Studies, The University of Texas, Austin, Texas 78712, USA

(Received 14 January 2008; accepted 19 March 2008; published online 30 April 2008)

This paper describes a magnetic nozzle with a magnetic mirror configuration that transforms a collisionless subsonic plasma flow into a supersonic jet expanding into the vacuum. The nozzle converts electron thermal energy into the ion kinetic energy via an ambipolar electric field. The ambipolar potential in the expanding plume involves a time-dependent rarefaction wave. Travelling through the rarefaction wave, electrons lose some kinetic energy and can become trapped downstream from the mirror throat. This work presents a rigorous adiabatic description of the trapped electron population. It examines the impact of the adiabatic cooling of the trapped electrons on the ambipolar potential and the ensuing ion acceleration. The problem is formulated for an arbitrary incoming electron distribution and then a "water-bag" electron distribution is used to obtain a closed-form analytical solution. © *2008 American Institute of Physics*.
[DOI: 10.1063/1.2907786]

I. INTRODUCTION

Supersonic plasma jets for space-propulsion applications[1,2] can be produced in a magnetic nozzle with a converging-diverging applied magnetic field (magnetic mirror).[3] The converging part of the nozzle accelerates an incoming subsonic flow, supplied by a plasma source, to the sonic speed. The flow becomes sonic at the nozzle throat, after which the acceleration continues in the diverging part of the nozzle. In this way, the magnetic plasma nozzle is similar to the conventional gas dynamic de Laval nozzle.[4]

As the flow velocity increases downstream, the plasma density drops and the electron mean free path with respect to electron-electron collisions increases. If the mean free path is much shorter than the nozzle, then the electrons are in a highly collisional regime. In this case, the electron distribution function is nearly Maxwellian and a fluid description fully applies.[5,6] The opposite case of a long mean free path requires a kinetic description.

In the case of cold incoming ions and hot electrons, the magnetic nozzle converts the electron thermal energy into kinetic energy of the ion motion along the magnetic field lines. The process involves an ambipolar electric field that balances an electron pressure gradient. The ambipolar field impedes electron motion in the downstream direction maintaining plasma quasineutrality. At the same time, it accelerates plasma ions pulling them downstream.

An interesting feature of the kinetic regime is that the magnetic mirror can limit direct access of electrons coming from the plasma source to certain areas of phase space in the downstream flow. Some electron trajectories that start upstream from the mirror return to the plasma source before they reach the mirror throat. Likewise, there are electron trajectories that always stay on the other side of the magnetic mirror. These trajectories correspond to electrons trapped downstream and, therefore, they are not directly accessible to the electrons produced by the source. This indicates that the corresponding areas of phase space may become depleted.

In plasma confinement systems, such as mirror machines, the directly inaccessible trajectories can be repopulated due to Coulomb collisions even in the kinetic regime.[7,8] The nearly steady-state plasma flow between the mirror and the end wall has a much longer time scale than the time between the collisions. This gives the collisions enough time to generate a population of trapped electrons downstream from the mirror.

In this paper, we address a different purely collisionless mechanism of electron trapping that might play an important role in plasma space applications such as plasma thrusters.[1,2] The key difference between a space thruster and a laboratory mirror machine is that a thruster produces a freely expanding plasma flow. On the other hand, a mirror machine has an end wall that creates a Debye sheath. The sheath reflects most of the incident electrons to keep the electron and ion fluxes to the wall equal. As a result, the wall enables the plasma electrons to establish a steady-state ambipolar potential profile inside the machine, with a steady-state sheath at the wall. In contrast, the ambipolar potential in an expanding plume ejected by a thruster is necessarily time-dependent. Its profile usually consists of two parts in the case of a supersonic flow: a steady-state part adjacent to the thruster and a rarefaction wave at the periphery.

The rarefaction wave accommodates a part of the total potential drop needed to keep electrons and ions together. Bouncing back and forth along the magnetic field lines, some electrons travel through both the steady-state area and the rarefaction wave. These electrons lose a part of their kinetic energy associated with the motion along the field lines while moving in the time-dependent field of the wave. The energy loss is entirely due to the fact that the whole wave structure is moving away from the thruster. As a result of the energy losses, electrons can become trapped downstream from the magnetic mirror. Once trapped, they cool down via the same mechanism, filling up the areas of phase space that would be inaccessible otherwise. The cooling is essentially adiabatic because the electron motion is much faster than the time

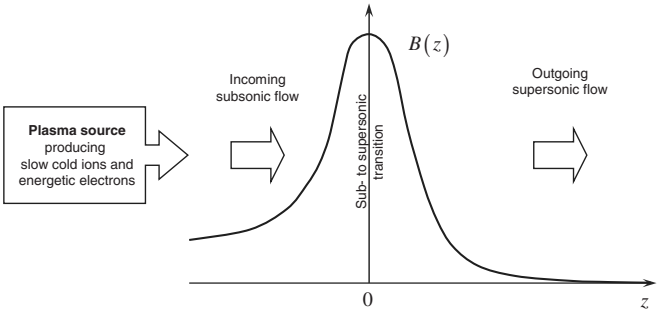

FIG. 1. Magnetic field profile along the axis of the magnetic nozzle and the plasma flow configuration.

evolution of the electrostatic potential (the latter is determined by the ion motion).

In this work, we present an accurate adiabatic description of the trapped electron population. We also examine the impact of the adiabatic cooling on the profile of the ambipolar potential and the ensuing ion acceleration. This problem can be formulated for an arbitrary distribution function of incoming electrons. However, in order to make the problem fully tractable analytically, we consider an incoming "water-bag" electron distribution.

The rest of the paper is organized as follows: Sec. II presents the main assumptions and key qualitative features of the model. Section III formulates the governing equations for an arbitrary distribution function of incoming electrons. In Sec. IV, we limit our consideration to a flow with a water-bag distribution of the incoming electrons and construct a rigorous analytical solution. Finally, Sec. V summarizes the results and gives concluding remarks.

II. QUALITATIVE PICTURE

We consider a collisionless plasma flow through an axisymmetric magnetic nozzle. The nozzle magnetic field is shown schematically in Fig. 1. We assume that a plasma source at the nozzle entrance creates a subsonic incoming flow. Instead of modeling the source explicitly, we simulate it by specifying time-independent distribution functions of incoming ions and electrons.

The plasma flow is governed by the guiding magnetic field and the ambipolar electric field. We simplify the flow description by assuming that the plasma ions are cold and that the flow is paraxial. The first assumption allows us to neglect the ion gyromotion. The second assumption allows us to treat the ambipolar electric field as being parallel to the magnetic field, making the problem effectively one-dimensional.

We seek a solution in which the ions accelerate progressively along the magnetic field lines. This implies that the ambipolar potential φ is a monotonically decreasing function of the axial coordinate z. Time evolution of the ambipolar potential is determined by the ion motion. Since the electron motion along the magnetic field lines is much faster than the ion motion, we regard the time evolution of φ as adiabatic in the context of electron dynamics.

The energy of electrons moving in this time-dependent potential is not conserved, because of a small energy loss that occurs during their motion through the rarefaction wave. The plasma source restores the energy of the returning electrons, but the trapped electrons are decoupled from the source and undergo the adiabatic cooling. The number of trapped electrons grows in time as the plasma continues to expand downstream and new incoming electrons become trapped.

Based on this picture, we use two different approximations for passing and trapped electrons. For passing electrons (those that return to the plasma source), we neglect the energy losses and treat them as if they were moving in a steady-state potential. The energy of a passing electron is then conserved in our model. For trapped electrons (those that bounce between the mirror and the rarefaction wave), the energy decreases with time, but the adiabatic invariant associated with the longitudinal motion remains conserved.

In addition to the aforementioned conservation laws, the magnetic moment of every electron is also conserved. It is then convenient to present the energy ε of an electron in the form,

$$\varepsilon = \tfrac{1}{2} m_e v_\parallel^2 + U_{\mathrm{eff}}, \tag{1}$$

where

$$U_{\mathrm{eff}} \equiv \mu B(z) - |e|\varphi(z;t), \tag{2}$$

is an effective potential for one-dimensional motion along the magnetic field and

$$\mu = \frac{m_e v_\perp^2}{2B} \tag{3}$$

is the magnetic moment. In Eqs. (1)–(3), m_e is the electron mass, e is the electron charge, and $v_\parallel$ and $v_\perp$ are the components of the electron velocity parallel and perpendicular to the magnetic field B. The magnetic field term in Eq. (2) accounts for the conversion of electron gyromotion into longitudinal motion in a nonuniform magnetic field.

Upstream from the mirror, the effective potential increases monotonically along the flow ($\partial U_{\mathrm{eff}}/\partial z > 0$) for all values of μ, because $\partial B/\partial z > 0$. Downstream from the mirror, the effective potential remains monotonically increasing for sufficiently small values of μ. However, it is nonmonotonic and has a local maximum (a peak) for large values of μ because of the decreasing magnetic term in Eq. (2). The location of the maximum z_* depends on μ and it is determined by the conditions $U'_{\mathrm{eff}}(z_*,\mu)=0$ and $U''_{\mathrm{eff}}(z_*,\mu)<0$. For a given magnetic moment, only electrons with $\varepsilon > U_{\mathrm{eff}}(z_*,\mu)$ can travel over the peak. It then follows that downstream from the peak the areas of phase space with $U_{\mathrm{eff}}(z_*,\mu) > \varepsilon \geqslant U_{\mathrm{eff}}(z,\mu)$ are inaccessible to passing electrons with magnetic moment μ.

In order to illustrate how an incoming electron becomes trapped downstream from the magnetic mirror, we consider an electron with magnetic moment μ moving in an effective potential U_{eff} shown in Fig. 2. This structure of U_{eff} is typical to a supersonic flow, as it has a steady-state part and a time evolving part (a barrier) that is moving away downstream.

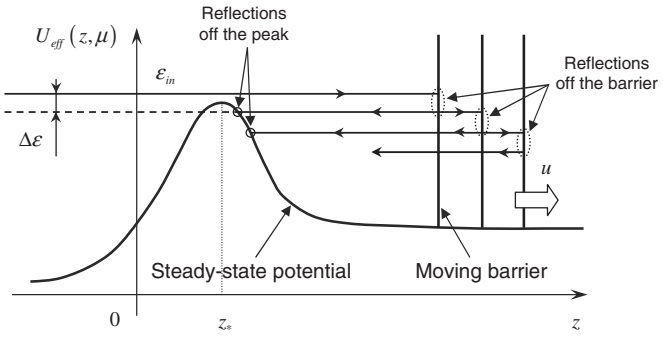

FIG. 2. Trapping of an incoming electron and its subsequent cooling.

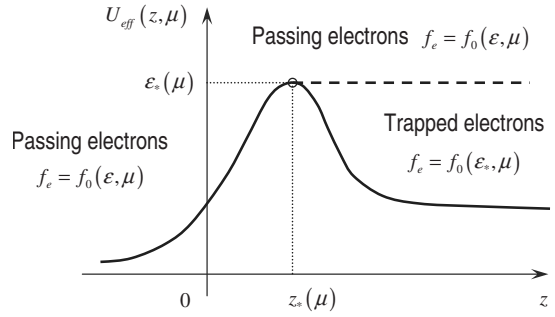

FIG. 3. Electron distribution for a given magnetic moment μ upstream and downstream from a peak.

The moving barrier here represents the rarefaction wave. As shown in Fig. 2, the incoming electron goes over the top of the peak and reflects off the moving barrier. As a result, the absolute value of the parallel electron velocity decreases by $2u$, where u is the barrier velocity. The corresponding decrease in the electron energy is $\Delta\varepsilon=2m_e u(v_1-u)$, where v_1 is the electron velocity prior to the reflection. The magnetic moment is nevertheless conserved by the reflection, so that the steady-state part of $U_{\rm eff}$ remains unchanged. Therefore, the electron is unable to return to the plasma source if $\varepsilon_{\rm in}-\Delta\varepsilon<U_{\rm eff}(z_*,\mu)$. It becomes trapped downstream from the mirror, bouncing back and forth between the peak and the barrier. The electron energy continues to decrease with every reflection off the moving barrier. This process can be described as adiabatic cooling as long as the characteristic electron velocity significantly exceeds u.

III. FORMULATION OF THE MODEL

The dynamics of a quasineutral paraxial plasma flow is governed by the following equations:

$$\frac{\partial V}{\partial t}+V\frac{\partial V}{\partial z}=-\frac{|e|}{m_i}\frac{\partial\varphi}{\partial z}, \tag{4}$$

$$\frac{\partial n}{\partial t}+B\frac{\partial}{\partial z}\left(\frac{nV}{B}\right)=0, \tag{5}$$

where V is the ion velocity that is directed along $\mathbf{B}$, m_i is the ion mass, n is the plasma density, and φ is the electrostatic potential. Equation (4) is the ion momentum balance equation and Eq. (5) is the ion continuity equation. We explicitly used the paraxiality of the magnetic field in Eqs. (4) and (5) by writing the derivative along the magnetic field lines as $\partial/\partial z$. A closed system of equation for V, n, and φ requires one more equation in addition to Eqs. (4) and (5). The remaining equation in our model is the quasineutrality condition $n=n_e$, where n_e is the electron density expressed in terms of φ.

In order to calculate the electron density, we need to express the local electron distribution function f_e in terms of the electron distribution function in the incoming flow. The incoming electrons are characterized by a given distribution $f_0(\varepsilon,\mu)$ defined for positive axial velocities $v_\parallel$. The total electron distribution at the nozzle entrance will also contain a nearly equal number of electrons moving in the opposite direction. The asymmetry in the total electron distribution function is very small because the plasma flow velocity is much smaller than the electron thermal velocity. We therefore neglect this asymmetry and set $f_0(-v_\parallel)=f_0(v_\parallel)$, so that the electron distribution in the incoming flow is $f_e=f_0(\varepsilon,\mu)$ for both positive and negative values of $v_\parallel$. The total energy ε and magnetic moment μ of each passing electron are conserved in our model. As a result, the expression $f_e=f_0(\varepsilon,\mu)$ remains valid downstream from the nozzle entrance in the areas of phase space accessible to passing electrons. In the case of a trapped electron, the integrals of motion are the magnetic moment μ and the adiabatic invariant I associated with the longitudinal motion. Consequently, the distribution function of trapped electrons is constant in both space and time if it is written in terms of μ and I (but not in terms of μ and ε).

In order to determine the distribution function of trapped electrons, we consider electrons that have the same magnetic moment μ. All such electrons are characterized by the same profile of $U_{\rm eff}$. If $U_{\rm eff}$ has a peak at $z=z_*$, then the electron distribution function for $z>z_*$ includes both passing and trapped electrons, as shown in Fig. 3. Electrons with $\varepsilon\geqslant\varepsilon_*(\mu)$ are passing electrons, whereas electrons with $\varepsilon<\varepsilon_*(\mu)$ are trapped electrons, where $\varepsilon_*(\mu)\equiv U_{\rm eff}(z_*,\mu)$. For passing electrons $[\varepsilon\geqslant\varepsilon_*(\mu)]$, the distribution is given by $f_e=f_0(\varepsilon,\mu)$. For trapped electrons $[\varepsilon<\varepsilon_*(\mu)]$, the distribution turns out to be $f_e=f_0[\varepsilon_*(\mu),\mu]$. We assume that $U_{\rm eff}$ has a steady state profile for $z\leqslant z_*$. Then the distribution function of the incoming electrons that become trapped is $f_0[\varepsilon_*(\mu),\mu]$, because the trapping occurs always at the same energy $\varepsilon=\varepsilon_*(\mu)$. Even though $\varepsilon_*(\mu)$ remains constant in time, the value of the adiabatic invariant I that corresponds to $\varepsilon_*(\mu)$ gradually increases due to the flow expansion. Once trapped, electrons cool down losing their energy, but conserving the adiabatic invariant. As a result, the distribution function of all trapped electrons with the same value of μ is equal to the time-independent distribution function of the passing electrons with energy $\varepsilon=\varepsilon_*(\mu)$. The phase space occupied by the trapped electrons is defined by the condition $\varepsilon_*(\mu)>\varepsilon\geqslant U_{\rm eff}(z,\mu)\equiv\mu B-|e|\varphi$ for $z>z_*$.

The electron density is then given by the following expression:

$$n = \pi B\left(\frac{2}{m_e}\right)^{3/2}\int_0^\infty d\mu\Bigg\{H[z_*(\mu)-z]\times\int_{\mu B-|e|\varphi}^\infty \frac{f_0(\varepsilon,\mu)d\varepsilon}{\sqrt{\varepsilon-\mu B+|e|\varphi}} + H[z-z_*(\mu)]\times\Bigg[\int_{\varepsilon_*(\mu)}^\infty \frac{f_0(\varepsilon,\mu)d\varepsilon}{\sqrt{\varepsilon-\mu B+|e|\varphi}} + \int_{\mu B-|e|\varphi}^{\varepsilon_*(\mu)} \frac{f_0[\varepsilon_*(\mu),\mu]d\varepsilon}{\sqrt{\varepsilon-\mu B+|e|\varphi}}\Bigg]\Bigg\}, \tag{6}$$

where H is the Heaviside step function. The first two terms are the passing electron contributions and the last term is the trapped electron contribution. Only the first term in Eq. (6) should be used for those values of μ that have a monotonically increasing profile of U_{eff} without a peak. Equation (6) defines n as a nonlocal functional of φ and B.

Equations (4)–(6) need to be solved together to find self-consistent profiles of the electrostatic potential and plasma density. In general, this would require a numerical procedure, but the development of such a procedure goes beyond the scope of this work. In what follows, we limit our consideration to a flow with a "water-bag" distribution of the incoming electrons, which allows us to construct a rigorous analytic solution of Eqs. (4)–(6).

IV. PLASMA FLOW WITH A WATER-BAG ELECTRON DISTRIBUTION

We choose a water-bag electron distribution at the nozzle entrance, such that

$$f_0(\varepsilon,\mu) = \frac{3n_{\text{in}}}{4\pi}\left(\frac{m_e}{2\varepsilon_{\text{in}}}\right)^{3/2} H(\varepsilon_{\text{in}}-\varepsilon), \tag{7}$$

where ε_{in} is the cutoff electron kinetic energy and n_{in} is the plasma density in the incoming flow. We also choose the electrostatic potential to be equal to zero at the nozzle entrance.

A. Steady-state flow in the converging part of the nozzle

We look for a self-consistent steady-state flow configuration upstream from the mirror. According to Eq. (6), the plasma density upstream from the mirror where all electrons are passing electrons, is given by

$$n = \frac{3}{4}\frac{n_{\text{in}}B}{\varepsilon_{\text{in}}^{3/2}}\int_0^{(\varepsilon_{\text{in}}+|e|\varphi)/B} d\mu\int_{\mu B-|e|\varphi}^{\varepsilon_{\text{in}}}\frac{d\varepsilon}{\sqrt{\varepsilon-\mu B+|e|\varphi}}. \tag{8}$$

The upper limit in the integral over μ is determined by the condition that $v_\parallel=0$ for $\varepsilon=\varepsilon_{\text{in}}$. A straightforward evaluation of the integrals in Eq. (8) gives

$$n = n_{\text{in}}\left(1+\frac{|e|\varphi}{\varepsilon_{\text{in}}}\right)^{3/2}. \tag{9}$$

In a steady-state flow, Eqs. (4) and (5) reduce to

$$\tfrac{1}{2}m_iV^2 + |e|\varphi = \tfrac{1}{2}m_iV_{\text{in}}^2, \tag{10}$$

$$\frac{nV}{B} = \frac{n_{\text{in}}V_{\text{in}}}{B_{\text{in}}}, \tag{11}$$

where V_{in} and B_{in} are the ion velocity and magnetic field at the nozzle entrance. We combine Eqs. (9)–(11) to find that

$$\frac{B^2}{B_{\text{in}}^2} = \left(1+\frac{|e|\varphi}{\varepsilon_{\text{in}}}\right)^3\left(1-\frac{2|e|\varphi}{m_iV_{\text{in}}^2}\right). \tag{12}$$

It follows from Eq. (12) that

$$\frac{2B}{B_{\text{in}}^2}\frac{\varepsilon_{\text{in}}}{|e|}\frac{dB}{d\varphi} = \frac{2}{m_iV_{\text{in}}^2}\left(1+\frac{|e|\varphi}{\varepsilon_{\text{in}}}\right)^2\left(\frac{3}{2}m_iV_{\text{in}}^2 - 4|e|\varphi - \varepsilon_{\text{in}}\right). \tag{13}$$

The derivative $d\varphi/dB$ is negative at the nozzle entrance ($\varphi=0$) if the incoming ions are sufficiently slow, such that

$$\frac{1}{2}m_iV_{\text{in}}^2 < \frac{\varepsilon_{\text{in}}}{3}. \tag{14}$$

In this case, the ions accelerate towards the nozzle throat. At

$$\varphi = \frac{3}{4|e|}\left(\frac{1}{2}m_iV_{in}^2 - \frac{\varepsilon_{\text{in}}}{3}\right), \tag{15}$$

the ion velocity becomes equal to the local speed of sound

$$C_s(\varphi) = \sqrt{\frac{2(\varepsilon_{\text{in}}+|e|\varphi)}{3m_i}} \tag{16}$$

and further flow acceleration is impossible in a converging magnetic field, because $d\varphi/dB$ changes sign [see Eq. (13)]. The expression for C_s can be derived by considering propagation of short-scale perturbations in a steady-state flow. Apparently, condition (14) is equivalent to the requirement that the incoming flow is subsonic [$V_{\text{in}}<C_s(0)$].

A smooth sub- to supersonic transition is possible only at the magnetic mirror throat, and it imposes the following constraint on the flow parameters:

$$\frac{B_0}{B_{\text{in}}} = \frac{3\sqrt{3}}{16}\sqrt{\frac{2\varepsilon_{\text{in}}}{m_iV_{\text{in}}^2}}\left(1+\frac{m_iV_{\text{in}}^2}{2\varepsilon_{\text{in}}}\right)^2, \tag{17}$$

where B_0 is the magnetic field at the mirror throat. Equation (17) is obtained from Eq. (12) using the condition that the electrostatic potential φ at the mirror throat is given by Eq. (15).

For the purpose of the subsequent analysis, we introduce

$$\varphi_0 \equiv \frac{3}{4|e|}\left(\frac{1}{2}m_iV_{\text{in}}^2 - \frac{\varepsilon_{\text{in}}}{3}\right), \tag{18}$$

$$\varepsilon_0 \equiv \varepsilon_{\text{in}} + |e|\varphi_0, \tag{19}$$

$$\tfrac{1}{2}m_iV_0^2 \equiv \tfrac{1}{2}m_iV_{\text{in}}^2 - |e|\varphi_0, \tag{20}$$

$$\Phi \equiv \varphi - \varphi_0. \tag{21}$$

The subscript "0" refers to the location of the mirror throat. The quantities φ_0, ε_0, and $m_iV_0^2/2$ are the corresponding electrostatic potential, the maximum electron kinetic energy, and the ion kinetic energy. It follows from Eqs. (15) and (18)–(21) that

$$\frac{1}{2}m_iV_0^2=\frac{\varepsilon_0}{3}. \tag{22}$$

We can now rewrite Eq. (12) in terms of the quantities associated with the mirror throat,

$$\frac{B}{B_0}=\left(1+\frac{|e|\Phi}{\varepsilon_0}\right)^{3/2}\left(1-3\frac{|e|\Phi}{\varepsilon_0}\right)^{1/2}. \tag{23}$$

B. Steady-state flow in the diverging part of the nozzle

Equation (23) holds at the mirror throat and in the adjacent diverging part of the nozzle as long as the plasma flow contains no trapped electrons. In the case of the water-bag distribution, the trapping of electrons with magnetic moment μ requires a peak in $U_{\mathrm{eff}}(z,\mu)$, with $\varepsilon_*(\mu)\leqslant\varepsilon_{\mathrm{in}}$. The trapping cannot occur at $\varepsilon_*(\mu)>\varepsilon_{\mathrm{in}}$, because there are no incoming electrons with energies above the cutoff energy $\varepsilon_{\mathrm{in}}$. The spatial boundary of the trapped electron population is determined by the location of the peak whose height is equal to $\varepsilon_{\mathrm{in}}$. The conditions that define this peak are

$$\mu B-|e|\Phi=\varepsilon_0, \tag{24}$$

$$\mu\frac{dB}{d\Phi}-|e|=0, \tag{25}$$

where B and Φ are related by Eq. (23). In what follows, we mark all quantities associated with the peak by subscript t. We find from Eqs. (23)–(25) that

$$B_t\equiv\frac{4}{3\sqrt{3}}B_0, \tag{26}$$

$$\Phi_t\equiv-\frac{\varepsilon_0}{3|e|}, \tag{27}$$

$$\mu_t\equiv\frac{\sqrt{3}}{2}\frac{\varepsilon_0}{B_0}. \tag{28}$$

It is straightforward to check that U_{eff} peaks downstream from the mirror throat for any μ greater than μ_t. All these peaks are located between $B=B_0$ and $B=B_t<B_0$ and their height exceeds the electron cutoff energy. This confirms that the region between $B=B_0$ and $B=B_t$ contains only passing electrons.

We now return to Eq. (6) to calculate the trapped electron contribution to the electron density for $B\leqslant B_t$. In the case of a water-bag distribution, the integrals in the square brackets in Eq. (6) can be combined into a single integral, eliminating the need to know the energy $\varepsilon_*(\mu)$ for every μ. We conjecture that $U_{\mathrm{eff}}(z,\mu_t)\leqslant\varepsilon_{\mathrm{in}}$ for $B\leqslant B_t$, such that $\mu\in[0,\mu_t]$ for $B\leqslant B_t$. The ensuing solution validates this conjecture (see Fig. 3). The electron density for $B\leqslant B_t$ is then given by

$$n=\frac{3}{4}\frac{n_{\mathrm{in}}B}{\varepsilon_{\mathrm{in}}^{3/2}}\int_0^{\mu_t}d\mu\int_{\mu B-|e|\varphi}^{\varepsilon_{\mathrm{in}}}\frac{d\varepsilon}{\sqrt{\varepsilon-\mu B+|e|\varphi}}. \tag{29}$$

We evaluate the integrals in Eq. (29) and use definitions (19) and (21) to find that

$$n=n_0\left[\left(1+\frac{|e|\Phi}{\varepsilon_0}\right)^{3/2}-\left(1+\frac{|e|\Phi}{\varepsilon_0}-\frac{\sqrt{3}}{2}\frac{B}{B_0}\right)^{3/2}\right], \tag{30}$$

where

$$n_0\equiv n_{\mathrm{in}}\left(1+\frac{|e|\varphi_0}{\varepsilon_{\mathrm{in}}}\right)^{3/2} \tag{31}$$

is the plasma density at the magnetic throat. The second bracket in Eq. (30) vanishes for $B\to B_t$, indicating that n is continuous at $B=B_t$.

Upstream from $B=B_t$, the electron density is given by the first term in the square brackets in Eq. (30) [see Eq. (9)]. Therefore, Eq. (30) can be extended from $B\leqslant B_t$ to $B_0\geqslant B\geqslant 0$ by including a multiplier $H(B_t-B)$ in front of the last term in the square brackets. We now combine Eqs. (10), (11), and (30) and use definitions (19)–(21) and (31) to find the following relation between Φ and B:

$$\frac{B}{B_0}=\left[\left(1+\frac{|e|\Phi}{\varepsilon_0}\right)^{3/2}-H(B_t-B)\left(1+\frac{|e|\Phi}{\varepsilon_0}-\frac{\sqrt{3}}{2}\frac{B}{B_0}\right)^{3/2}\right]\times\left(1-3\frac{|e|\Phi}{\varepsilon_0}\right)^{1/2}. \tag{32}$$

According to Eq. (32), the electrostatic potential decreases monotonically with B. For $B\to 0$, the potential Φ converges to

$$\Phi_f\equiv-\frac{3+2\sqrt{5}}{9}\frac{\varepsilon_0}{|e|}\approx-0.83\frac{\varepsilon_0}{|e|}. \tag{33}$$

Indeed, expanding the right-hand side of Eq. (32) in B/B_0 and keeping the lowest order term, we obtain

$$\frac{3\sqrt{3}}{4}\left(1+\frac{|e|\Phi}{\varepsilon_0}\right)^{1/2}\left(1-3\frac{|e|\Phi}{\varepsilon_0}\right)^{1/2}=1. \tag{34}$$

Expression (33) represents the negative root of this equation.

Asymptotically, Eq. (32) describes a freely expanding steady-state plasma flow. The ion kinetic energy in this flow is

$$\frac{1}{2}m_iV_f^2=\frac{6+2\sqrt{5}}{9}\varepsilon_0\approx 1.2\varepsilon_0. \tag{35}$$

This energy is greater than the maximum kinetic energy of the electrons at the mirror throat.

Figure 4 shows steady-state profiles of $U_{\mathrm{eff}}=\mu B-|e|\varphi$ downstream from the mirror for several different values of the magnetic moment μ. The solid curves correspond to the self-consistent solution (32). The behavior of the solid curves in Fig. 4 shows that a passing electron that goes over a peak does not turn around in the steady-state part of the flow. Trapped electrons travelling downstream also do not turn around in the steady-state part of the flow, because U_{eff} decreases monotonically downstream from a peak. The reflec-

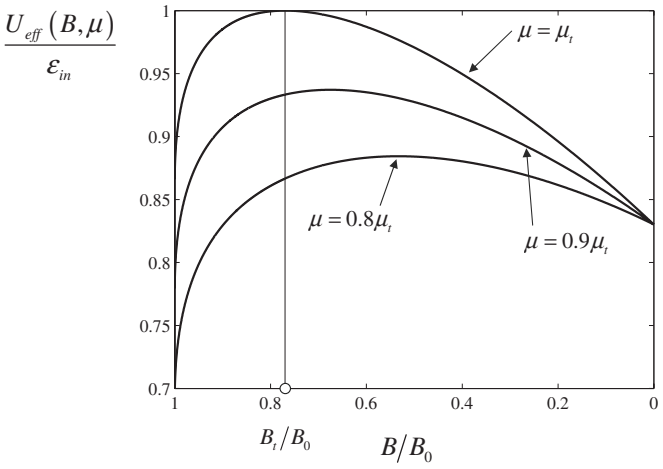

FIG. 4. Profiles of $U_{\text{eff}}=\mu B-|e|\varphi$ downstream from the mirror for three different values of the magnetic moment $(0.8\mu_t, 0.9\mu_t, \mu_t)$. The electrostatic potential φ is related to the magnetic field B through Eq. (32).

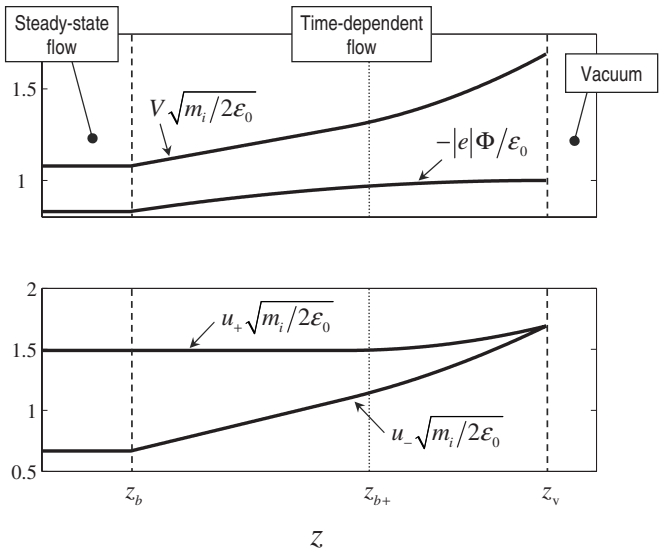

FIG. 5. Plasma flow configuration in the low magnetic field area.

tion of all these electrons must take place in the time-dependent part of the flow that accommodates the potential drop needed to keep electrons and ions together. If the time-dependent part is entirely in the area with a very low magnetic field, then the corresponding potential drop is equal to $\varepsilon_0/|e|+\Phi_f$.

C. Time-dependent flow in the diverging part of the nozzle

Even prior to finding the exact solution, it is clear that the boundary between the steady-state and the time-dependent flows should be moving away from the mirror throat, since the plasma flow is supersonic. Therefore, the entire time-dependent part of the flow eventually shifts to the area of very low magnetic field. In this case, the electrons in the time-dependent area have a negligibly small gyroenergy and their dynamics is primarily governed by the electric field. In what follows, we employ this simplification to construct an analytical solution of the flow equations.

The flow pattern under consideration is shown in Fig. 5. The time-dependent flow borders the steady-state flow at a moving boundary located at $z=z_b(t)$. We require that $B/B_0 \ll 1+|e|\Phi_f/\varepsilon_0$ at $z=z_b(t)$, such that the steady-state flow at $z=z_b$ is essentially force-free, with $\Phi\approx\Phi_f$ and $V\approx V_f$. Therefore, the function Φ varies inside the time-dependent flow from $\Phi=\Phi_f$ at $z=z_b(t)$ to $\Phi=-\varepsilon_0/|e|$ at the plasma-vacuum boundary, whose location we denote as $z_v(t)$.

For $B/B_0 \ll 1+|e|\Phi/\varepsilon_0$, the electron density given by Eq. (30) can be approximated as

$$n \approx n_0 \frac{3\sqrt{3}}{4}\frac{B}{B_0}\left(1+\frac{|e|\Phi}{\varepsilon_0}\right)^{1/2}. \tag{36}$$

We use this expression to eliminate n from Eqs. (4) and (5), which gives

$$\frac{\partial V}{\partial t}+V\frac{\partial V}{\partial z}=-\frac{\varepsilon_0}{m_i}\frac{\partial}{\partial z}\left(1+\frac{|e|\Phi}{\varepsilon_0}\right), \tag{37}$$

$$\frac{\partial}{\partial t}\left(1+\frac{|e|\Phi}{\varepsilon_0}\right)^{1/2}+\frac{\partial}{\partial z}\left[V\left(1+\frac{|e|\Phi}{\varepsilon_0}\right)^{1/2}\right]=0. \tag{38}$$

We now replace V and Φ by more convenient unknown functions

$$u_\pm \equiv V \pm \sqrt{\frac{2\varepsilon_0}{m_i}}\left(1+\frac{|e|\Phi}{\varepsilon_0}\right)^{1/2}, \tag{39}$$

which transforms Eqs. (37) and (38) into two decoupled equations,

$$\left[\frac{\partial}{\partial t}+u_\pm\frac{\partial}{\partial z}\right]u_\pm=0. \tag{40}$$

For a set of given profiles $V(z,\tilde{t})$ and $\Phi(z,\tilde{t})$ at a time moment $\tilde{t}$, Eqs. (40) allow us to find the flow dynamics at $t>\tilde{t}$. The time $\tilde{t}$ must be sufficiently large for the profiles to satisfy the condition $B[z_b(\tilde{t})]/B_0 \ll 1+|e|\Phi_f/\varepsilon_0$. The profiles $V(z,\tilde{t})$ and $\Phi(z,\tilde{t})$ are determined by the flow evolution at $t<\tilde{t}$, involving the time-dependent flow through the mirror. As shown below, the effect of the intermediate dynamics diminishes with time and vanishes at $t\to\infty$ [see Eqs. (47) and (48)].

Equations (39) give the initial conditions $u_+(z,\tilde{t})$ and $u_-(z,\tilde{t})$ corresponding to $V(z,\tilde{t})$ and $\Phi(z,\tilde{t})$. The resulting solutions of Eqs. (40) at $t>\tilde{t}$ are given implicitly by

$$u_\pm(z,t)=G_\pm[z-(t-\tilde{t})u_\pm(z,t)], \tag{41}$$

where $G_\pm(z)\equiv u_\pm(z,\tilde{t})$. For the force-free steady-state flow, with $\Phi=\Phi_f$ and $V=V_f$, we have

$$u_\pm=u_{f\pm}\equiv\frac{1}{3}\sqrt{\frac{2\varepsilon_0}{m_i}}[(6+2\sqrt{5})^{1/2}\pm(6-2\sqrt{5})^{1/2}]. \tag{42}$$

Both of these values are positive, and we require that $G_+(z)$ and $G_-(z)$ satisfy the condition $dG_\pm/dz\geq 0$ to avoid steepening of the solutions with time.

Initially, u_+ and u_- match the solution given by Eqs. (42) at $z_{b\pm}(\tilde{t})=z_b(\tilde{t})$. Later in time, the matching points move according to Eqs. (41), such that

$$z_{b\pm}(t) = z_b(\tilde{t}) + u_{f\pm}(t-\tilde{t}). \tag{43}$$

The matching points become separated at $t>\tilde{t}$, with $z_{b+}(t) > z_{b-}(t)$, because $u_{f+}>u_{f-}$. The boundary between the steady-state and the time-dependent flows is determined by $z_{b-}(t)$, such that $z_b(t)=z_{b-}(t)$, as shown in Fig. 5. Note that the boundary is moving away from the mirror throat since u_{f-} is positive.

The leading edge of the plasma flow is initially located at $z=z_v(\tilde{t})$, where $\Phi=-\varepsilon_0/|e|$. It then follows from Eqs. (39) that $u_+[z_v(\tilde{t})]=u_-[z_v(\tilde{t})]=V$. Therefore, the leading edge of u_+ and the leading edge of u_- move away from the mirror at the same rate equal to the velocity of the fastest ions $V_{\max}$. The electric field at the leading edge vanishes due to quasineutrality, so that the ions at the leading edge move without acceleration and $V_{\max}$ remains constant in time. We then find that

$$z_v(t) = z_v(\tilde{t}) + V_{\max}(t-\tilde{t}), \tag{44}$$

where $V_{\max}$ is an unknown quantity related to the initial conditions. The condition $dG_\pm/dz \geqslant 0$ implies that $V_{\max} \geqslant u_{f+}$.

The time-dependent areas in u_+ and u_- expand and shift downstream with time. At $t\to\infty$, Eqs. (43) and (44) reduce to $z_{b\pm}(t)\approx u_{f\pm}t$ and $z_v(t)\approx V_{\max}t$, and the time-dependent part of the solution (41) then evolves into the following self-similar solution:

$$u_\pm(z,t) = \frac{z}{t} H(z-u_{f\pm}t) H(V_{\max}t - z). \tag{45}$$

We can now obtain the asymptotic expressions for the flow velocity V and plasma density n. We use Eqs. (36) and (39) to find that

$$\frac{n}{n_0} = \frac{3\sqrt{3}}{4}\frac{B}{B_0}\sqrt{\frac{m_i}{2\varepsilon_0}}\frac{u_+-u_-}{2}. \tag{46}$$

It then follows from Eq. (45) that n vanishes at $z=u_{f+}t$, which means that the number of particles between $z=u_{f+}t$ and $z=V_{\max}t$ vanishes with time. The reason is that the boundary z_{b+} is moving faster than the ions at the same location and, as a result, it gradually overtakes ions in the downstream flow. The resulting asymptotic solution for the plasma flow in the low magnetic field region is given by

$$n = n_0\frac{3\sqrt{3}}{8}\frac{B}{B_0}\sqrt{\frac{m_i}{2\varepsilon_0}} \times\left[u_{f+} - u_{f-}H(u_{f-}t-z) - \frac{z}{t}H(z-u_{f-}t)\right]H(u_{f+}t-z), \tag{47}$$

$$V = V_f + \frac{z-u_{f-}t}{2t}H(z-u_{f-}t). \tag{48}$$

We observe that initial conditions do not affect the asymptotic structure of the plasma flow.

The asymptotic solution exhibits a rarefaction wave, whose inner and outer fronts propagate away from the mirror throat. The velocity of the inner wave front, u_{f-}, is smaller than the local ion velocity. Therefore, there is a continuous flux of new ions from the steady-state flow into the rarefaction wave. The ions then undergo additional acceleration by the electric field of the wave.

Using Eqs. (22), (36), and (48), and the conservation of the particle and magnetic fluxes, we find that the ratio of the ion flux Ψ_{wave} through the inner wave front to the ion flux Ψ_0 through the mirror throat is given by

$$\frac{\Psi_{\text{wave}}}{\Psi_0} = \frac{6-2\sqrt{5}}{4}. \tag{49}$$

Asymptotically, the number of ions in the rarefaction wave is $N_{\text{wave}}=\Psi_{\text{wave}}t$, whereas the number of ions in the steady-state flow downstream from the mirror throat is $N_{\text{steady}} =(\Psi_0-\Psi_{\text{wave}})t$. Therefore, the rarefaction wave contains a notable fraction of all the ions located downstream from the throat,

$$\frac{N_{\text{wave}}}{N_{\text{steady}}+N_{\text{wave}}} = \frac{\Psi_{\text{wave}}}{\Psi_0} \approx 0.4. \tag{50}$$

To conclude this section, we give the asymptotic expressions for the time derivatives of the total momentum P and kinetic energy K downstream from the mirror throat,

$$\frac{dP}{dt} = m_i V_0 \Psi_0 \left(2+\frac{\sqrt{5}}{3}\right)\left(2-\frac{2\sqrt{5}}{3}\right)^{1/2} \approx 2m_i V_0 \Psi_0, \tag{51}$$

$$\frac{dK}{dt} = \frac{4}{3}\varepsilon_0\Psi_0. \tag{52}$$

The total momentum P is the ion momentum, since the electron momentum is negligible in the adiabatic flow. The total kinetic energy K includes both the ion (K_i) and electron (K_e) contributions, but the ion contribution to this energy turns out to be much greater than the electron part,

$$\frac{dK_i/dt}{dK_e/dt} \approx 29. \tag{53}$$

V. SUMMARY AND CONCLUDING REMARKS

We have developed a self-consistent model that describes a quasineutral plasma flow in a nozzle with a magnetic mirror configuration. The model addresses a purely collisionless mechanism of electron trapping downstream from the mirror throat. The nozzle produces a freely expanding supersonic plasma jet with a force-free steady-state plasma flow adjacent to the magnetic mirror and a rarefaction wave at the leading edge of the jet. The rarefaction wave affects the electron distribution function by causing electron trapping and subsequent adiabatic cooling.

The electron trapping and cooling are robust features of a supersonic collisionless flow. We have considered a case of a water-bag incoming electron distribution in order to carry out all the calculations analytically. Using the model formu-

lated in Sec. III, it should be possible to solve the problem numerically for an arbitrary incoming electron distribution, including a Maxwellian distribution.

Even though the specific form of the solution depends on the electron distribution function, the presence of the rarefaction wave itself at the leading edge of the flow is a robust feature of a freely expanding supersonic flow. Such flow necessarily consists of two parts: a steady-state part adjacent to the thruster and a time dependent part (rarefaction wave) at the leading edge. The boundary between the steady-state and the time-dependent flows moves away from the thruster, since the flow is supersonic. However, relative to the flow, the boundary is moving upstream with the local sound speed. As a result, the number of ions in the rarefaction wave continuously increases, so that the wave contains a sizable fraction of all the ions downstream from the nozzle throat.

In our analysis, we have assumed a given magnetic field, thus neglecting the effect of the plasma flow on the magnetic configuration. This assumption is valid for a strong guiding magnetic field. However, the magnetic field significantly weakens downstream in the plume and, eventually, distortion of the magnetic field by the flow itself becomes important in determining the overall magnetic configuration. This issue is directly related to the problem of plasma detachment in space thrusters.[1,2,5,6,9–12]

Finally, we should mention that there are a number of papers that employ standard magnetohydrodynamics (MHD) to simulate magnetic nozzles. This approach assumes that the electron distribution remains Maxwellian downstream, which is justified only in a highly collisional flow. In many cases, particularly in the expanding plume, the electrons may become collisionless and under such conditions the MHD approximation is no longer valid. The use of the "standard" fluid description of the plasma electrons, as done in Ref. 13, ignores the effect of the trapped electron population. This approach should generally be replaced by a proper kinetic treatment of electrons.

ACKNOWLEDGMENTS

The authors thank Dr. Dmitri Ryutov for stimulating discussions and constructive comments.

This work is supported by Ad Astra Rocket Company and the U.S. Department of Energy under Contract No. DE-FG02-04ER-54742.

[1] F. R. Chang-Daz, Sci. Am. (Int. Ed.) **283**, 90 (2000).
[2] A. V. Arefiev and B. N. Breizman, Phys. Plasmas **11**, 2942 (2004).
[3] S. A. Cohen, N. S. Siefert, S. Stange, R. F. Boivin, E. E. Scime, and F. M. Levinton, Phys. Plasmas **10**, 2593 (2003).
[4] L. D. Landau and E. M. Lifshitz, *Fluid Mechanics*, 2nd ed. (Pergamon, Oxford, 1979), p. 348.
[5] P. G. Mikellides, P. J. Turchi, and I. G. Mikellides, J. Propul. Power **18**, 146 (2002).
[6] I. G. Mikellides, P. G. Mikellides, P. J. Turchi, and T. M. York, J. Propul. Power **18**, 152 (2002).
[7] I. K. Konkashbaev, I. S. Landman, and F. R. Ulinich, Sov. Phys. JETP **47**, 501 (1978).
[8] D. D. Ryutov, Fusion Sci. Technol. **47**, 148 (2005).
[9] E. B. Hooper, J. Propul. Power **9**, 757 (1993).
[10] See National Technical Information Service Document No. DE00763033, R. A. Gerwin, G. J. Marklin, A. G. Sgro, and A. H. Glasser, LANL, Los Alamos, NM, AFOSR Technical Report No. AL-TR-89-092, "Characterization of Plasma Flow Through Magnetic Nozzles," 1990. Copies can be obtained from National Technical Information Service, Springfield, VA 22101.
[11] R. W. Moses, Jr., R. A. Gerwin, and K. F. Schoenberg, AIP Conf. Proc. **246**, 1293 (1992).
[12] A. V. Arefiev and B. N. Breizman, Phys. Plasmas **12**, 043504 (2005).
[13] R. Winglee, T. Ziemba, L. Giersch, J. Prager, J. Carscadden, and B. R. Roberson, Phys. Plasmas **14**, 063501 (2007).